Bichromatic excitation of coherent Raman beats in rare-earth solids

Tilo Blasberg and Dieter Suter
Institut für Quantenelektronik, ETH Zürich, CH-8093 Zürich, Switzerland
(Received 26 July 1994)

In coherent Raman beat experiments a laser field coherently scatters off a material excitation that evolves under the internal Hamiltonian of the system. The Raman signal, which is observed as a beat signal between the test laser and the scattered Raman field, provides information on energy-level splittings and dephasing rates. We propose a modification of this technique, which allows, in contrast to the conventional method, the excitation of coherent Raman beats also in systems with large sublevel splittings and small oscillator strengths. For this purpose, we use a bichromatic laser field to excite the coherent superposition in the medium. We calculate the evolution of the coherence during the laser excitation analytically and discuss its dependence on various experimental parameters. We compare the theoretical results with experimental data from Pr^{3+}:$YAlO_3$.

I. INTRODUCTION

Coherent Raman scattering[1] is an extension of conventional Raman spectroscopy that relies on the coupling between a laser field and a coherent excitation of the material. The presence of the excitation changes the scattering cross section for the Raman process qualitatively: the Raman field becomes linear in the incident test laser field and Stokes and anti-Stokes components occur with the same amplitude. The test laser, which scatters off the material excitation, must be (near-)resonant with an optical transition that shares an energy level with the transition in which the material excitation exists.

The enhanced cross section allows one to observe Raman scattering at low intensities. To achieve this increased coupling efficiency, however, one must first prepare the coherent excitation in the sample. This can be done continuously, using, e.g., resonant rf (Ref. 2) or microwave fields. For coherent Raman beat experiments, however, the coherent sample excitation is prepared before the actual Raman scattering process. The interference between the incident test laser field and the scattered Raman field on a quadratic photodetector produces a beat signal whose frequency is the sublevel transition frequency. During the Raman scattering process, the coherence decays under the influence of radiative decay and collision processes. The beat signal reflects this decay of the coherence. Coherent Raman beats contain, therefore, information on sublevel splittings and dynamic interactions in the sample. As we will see, their frequency resolution is not affected by laser frequency jitter and can be considerably better than the width of the optical resonance line. Coherent Raman beats have been used for high-resolution spectroscopy of atomic[3,4] and molecular[5,6] vapors.

Rare-earth ions in crystals represent another important class of materials, where coherent Raman beats have been employed successfully to study energy separations between nuclear spin states.[7] Optical transitions of rare-earth ions in crystals are *inhomogeneously* broadened with a typical linewidth of several gigahertz at cryogenic temperatures. On the other hand their *homogeneous* width can be less than 1 kHz.[8] Because of this high ratio between the two linewidths these crystals are interesting candidates for high-density optical data storage[9] using spectral hole burning.[10] Coherent Raman beat signals, which are insensitive to the inhomogeneous broadening, contain information on static and dynamic interactions. However, the weak transition strengths that are responsible for the narrow linewidths of rare-earth ions make the excitation of coherent Raman beats with conventional techniques difficult. For efficient excitation of the sublevel coherence, the optical Rabi frequency of the exciting laser pulse has to be greater than the sublevel splittings in the sample.[11] Coherent Raman beats could therefore only be observed in these systems when the sublevel splittings were of the order of less than a few megahertz.

This limitation can be circumvented by using a bichromatic laser field to excite the coherent superposition in the medium.[12] If the two frequency components of the pulse match the two optical transitions in a quantum-mechanical three-level system, the simultaneous interaction with both laser fields leads to a high excitation efficiency.

The paper is structured as follows. We start with a brief introduction to the principle of coherent Raman beat experiments. Afterwards we use a three-level model to describe the atomic system. We use this model to derive an analytical expression for the time evolution of the coherence, when the atom is driven by a bichromatic laser field. We discuss the dependence of the excitation efficiency on various experimental parameters and show how the bichromatic excitation overcomes the limitations of the conventional technique. Then we describe our experimental setup, which uses intensity-modulated pump pulses to create the bichromatic laser field. With this setup, we obtained experimental results that are in excellent agreement with the theoretical description of the scattering process.

0163-1829/95/51(10)/6309(10)/$06.00

II. COHERENT RAMAN BEAT EXPERIMENTS

For our discussion of the basic Raman beat experiment, we use the V-type three-level system represented at the bottom of Fig. 1. It consists of an electronic ground state $|1\rangle$ and two nondegenerate sublevels $|2\rangle$ and $|3\rangle$ of an electronically excited state. Optical transitions connect the ground state with both excited-state sublevels.

The coherent Raman beat experiment consists of two distinct periods. During a preparation period a pump laser pulse couples to the two optical transitions, as indicated by the two arrows, and excites a coherent superposition between the two excited states (wavy line in Fig. 1). During the detection period, a weak test laser beam, which is resonant with the transition $|1\rangle \leftrightarrow |3\rangle$, scatters off this excitation, creating a Raman field in the transition $|1\rangle \leftrightarrow |2\rangle$. The beat signal between the Raman field and the test laser field on a quadratic photodetector produces a signal that is directly proportional to the sublevel coherence ρ_{23}. Its frequency equals the sublevel transition frequency and its decay corresponds to the relaxation of the sample excitation.

For the excitation of the coherent superposition we use a bichromatic pump laser field. During the preparation period each component of the bichromatic laser field couples to one optical transition. As is well known from the theory of two-level atoms,[13] a laser field creates a coherent superposition between a ground and an excited state, if it couples to an optical transition between these two states. If a laser field has created a coherent superposition $c_1|\psi_1\rangle + c_2|\psi_2\rangle$ between the states $|1\rangle$ and $|2\rangle$ and a second laser field couples to the other optical transition $|1\rangle \leftrightarrow |3\rangle$, it transforms this state into

$$c_1|\psi_1\rangle + c_2|\psi_2\rangle \xrightarrow[\omega_{13}]{} c_1'|\psi_1\rangle + c_2|\psi_2\rangle + c_3'|\psi_3\rangle \ .$$

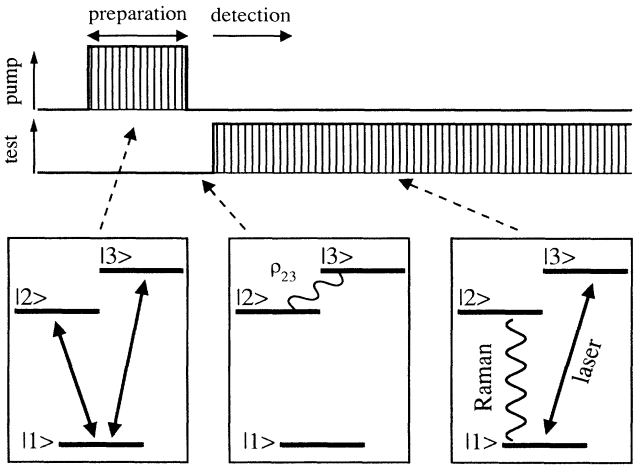

FIG. 1. Principle of coherent Raman beat experiments. During the preparation period, the pump laser pulse couples to the two optical transitions and excites a coherent superposition ρ_{23} of the excited states $|2\rangle$ and $|3\rangle$. During detection, the test laser beam scatters off the excited-state coherence, creating a Raman field.

This state contains coherence between all three states: apart from the two optical transitions, in which the laser pulses have excited coherence, there is also coherence in the third transition, which cannot be excited directly. Such a coherence results not only from the sequential application of two laser fields, as considered here, but also from their simultaneous application.

The separation of coherent Raman beat experiments into two different periods allows one to treat both processes independently of each other. In particular, the linear dependence of the Raman beat signal on the sublevel coherence allows one to study the excitation process without the need to discuss the detection process in detail. We use this possibility in the following section, where we discuss only the evolution of the sublevel coherence under the influence of the pump laser field.

III. THEORY

A. Bichromatic excitation of sublevel coherence

We calculate the time evolution for the V-type three-level system of Fig. 2. It consists of a single ground state $|1\rangle$ and two excited states $|2\rangle$ and $|3\rangle$. The frequency ω_0 refers to the energy separation between the ground state and the mean of the two excited states. In contrast to this optical frequency, the separation Δ between the two excited states is in the radio frequency range. While we discuss here only a V-type system, the technique is also applicable to Λ-type systems, as we will show in the experimental section.

For the Hamiltonian of the unperturbed system, we use the traceless operator

$$\mathcal{H}_0 = \hbar \begin{bmatrix} -\frac{2\omega_0}{3} & 0 & 0 \\ 0 & \frac{\omega_0}{3} - \frac{\Delta}{2} & 0 \\ 0 & 0 & \frac{\omega_0}{3} + \frac{\Delta}{2} \end{bmatrix} . \qquad (1)$$

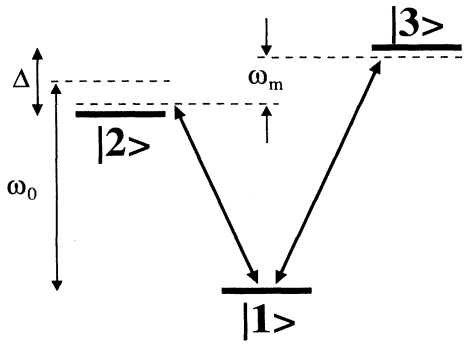

FIG. 2. Resonant interaction of a bichromatic laser field with a three-level atom in V configuration. Level $|1\rangle$ is an electronic ground state; levels $|2\rangle$ and $|3\rangle$ are nondegenerate sublevels of an electronically excited state, separated by the energy difference Δ. ω_0 is the mean excitation energy of the two excited states and ω_m is the frequency difference between the two field components.

We write the optical frequencies of the two components of the bichromatic laser field as $\omega_L \pm \omega_m/2$, where ω_L represents the laser frequency and ω_m the frequency difference between the two components. In the following, we assume that the laser frequency ω_L matches the energy difference ω_0 between the center of the two excited-state sublevels and the ground state: $\omega_L = \omega_0$. If at the same time the frequency difference ω_m matches the sublevel transition frequency Δ, the two components of the bichromatic laser field are resonant with the two optical transitions.

The optical Rabi frequency

$$\Omega_{1i} = \frac{\mu_{1i} E_0}{\hbar} \quad (i=2,3) \tag{2}$$

is proportional to the dipole matrix element and the electric field amplitude E_0 in the corresponding transition. As usual, we choose the phase of the eigenstates such that the matrix elements are real. If the optical Rabi frequency is small compared to the sublevel splitting, we only have to consider the coupling of one field component to each optical transition. The matrix elements of the coupling Hamiltonian are then

$$V_{1i}(t) = \langle 1|V(t)|i\rangle = \hbar\Omega_{1i}\cos[(\omega_0 \mp \tfrac{1}{2}\omega_m)t] , \tag{3}$$

with $i \in \{2,3\}$. Here the upper sign refers to the optical transition $|1\rangle \leftrightarrow |2\rangle$ and the lower sign to the transition $|1\rangle \leftrightarrow |3\rangle$. The total Hamiltonian is the sum of the static and the time-dependent Hamiltonians: $\mathcal{H} = \mathcal{H}_0 + V(t)$.

We make the Hamiltonian time independent by transforming it into an interaction representation defined by the unitary operator

$$U(t) = \begin{pmatrix} \exp\left[-i\frac{2\omega_0}{3}t\right] & 0 & 0 \\ 0 & \exp\left[i\left[\frac{\omega_0}{3} - \frac{\omega_m}{2}\right]t\right] & 0 \\ 0 & 0 & \exp\left[i\left[\frac{\omega_0}{3} + \frac{\omega_m}{2}\right]t\right] \end{pmatrix} . \tag{4}$$

The resulting interaction Hamiltonian in the rotating-wave approximation has the form

$$\mathcal{H}^r = U(t)\mathcal{H}U^{-1}(t) + i\dot{U}(t)U^{-1}(t) = \hbar \begin{pmatrix} 0 & \frac{\Omega_{12}}{2} & \frac{\Omega_{13}}{2} \\ \frac{\Omega_{12}}{2} & -\frac{\delta_m}{2} & 0 \\ \frac{\Omega_{13}}{2} & 0 & +\frac{\delta_m}{2} \end{pmatrix} , \tag{5}$$

where we have defined the sublevel detuning $\delta_m = \Delta - \omega_m$. At resonance ($\delta_m = 0$), all three levels are degenerate and the Hamiltonian contains only off-diagonal elements. In the general case ($\delta_m \neq 0$), the ground state $|1\rangle$ becomes centered between the two excited states.

B. Resonant excitation

We start the discussion with the doubly resonant case characterized by $\delta_m = 0$. The two components of the laser field are then resonant with the two optical transitions. We assume that the system is initially in thermal equilibrium and calculate the evolution of the coherence ρ_{23} between the two excited states.

To calculate the time evolution of the density matrix

$$\rho^r(t) = \exp(-i\mathcal{H}^r t)\rho^r(0)\exp(i\mathcal{H}^r t) , \tag{6}$$

we diagonalize the Hamiltonian $\mathcal{H}^r$, using the unitary transformation

$$U = U_2 U_1 = \frac{1}{\sqrt{2}} \begin{pmatrix} 1 & 1 & 0 \\ -1 & 1 & 0 \\ 0 & 0 & \sqrt{2} \end{pmatrix} \begin{pmatrix} 1 & 0 & 0 \\ 0 & \cos\frac{\Theta}{2} & \sin\frac{\Theta}{2} \\ 0 & -\sin\frac{\Theta}{2} & \cos\frac{\Theta}{2} \end{pmatrix} . \tag{7}$$

The rotation angle Θ is

$$\Theta = 2\tan^{-1}\left[\frac{\Omega_{13}}{\Omega_{12}}\right] . \tag{8}$$

The eigenvalues of the Hamiltonian are $0, \pm\Omega_e/2$, where $\Omega_e = \sqrt{\Omega_{12}^2 + \Omega_{13}^2}$ is an effective Rabi frequency.

If the system is initially in thermal equilibrium, the only nonvanishing density operator element is the ground-state population $\rho_{11} = 1$. Neglecting relaxation, we obtain the evolution of the excited-state coherence,

$$\rho_{23}(t) = \frac{\Omega_{12}\Omega_{13}}{\Omega_e^2}\sin^2\left[\frac{\Omega_e}{2}t\right] . \tag{9}$$

The imaginary part of the coherence vanishes. The effective Rabi frequency Ω_e determines the time scale on which the coherent superposition is created. For short pulse lengths the amplitude of the sublevel coherence increases quadratically with the interaction time.

The maximum amplitude of the sublevel coherence that can be excited depends only on the ratio of the two

optical Rabi frequencies Ω_{12} and Ω_{13}. Figure 3 shows this relation. The excitation is optimized when the two coupling strengths are equal, $\Omega_{12}=\Omega_{13}$, and decreases with increasing mismatch. The optical Rabi frequency depends on the field amplitude and on the oscillator strength of the corresponding optical transition. Hence the optimum condition for the excitation of sublevel coherence can always be realized with a bichromatic laser field by adjusting the field amplitudes of the two frequency components.

C. Difference-frequency mismatch

The excitation process changes when the two components of the laser field are not exactly resonant with the two optical transitions. For reasons that will become clear in the experimental section, we assume that the laser frequency matches the mean excitation energy, $\omega_L=\omega_0$, and discuss the excitation as a function of the difference-frequency mismatch δ_m. Furthermore, we assume that the two optical Rabi frequencies are equal ($\Omega_{12}=\Omega_{13}=\Omega_1$). With these assumptions, we can use the unitary transformation U

$$U=U_3U_2U_1$$

$$=\frac{1}{2}\begin{bmatrix}1&1&0\\-1&1&0\\0&0&\sqrt{2}\end{bmatrix}\begin{bmatrix}\cos\frac{\theta}{2}&0&\sin\frac{\theta}{2}\\0&1&0\\-\sin\frac{\theta}{2}&0&\cos\frac{\theta}{2}\end{bmatrix}\times\begin{bmatrix}\sqrt{2}&0&0\\0&1&1\\0&-1&1\end{bmatrix} \tag{10}$$

with the rotation angle

$$\theta=2\tan^{-1}\left[\frac{\delta_m}{\sqrt{2}\Omega_1}\right] \tag{11}$$

to diagonalize the Hamiltonian. Its eigenvalues are 0, $\pm\Omega_0/2$, with $\Omega_0=\sqrt{2\Omega_1^2+\delta_m^2}$.

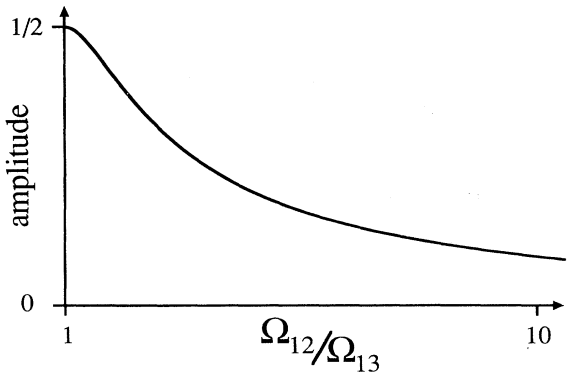

FIG. 3. Maximum amplitude of the sublevel coherence ρ_{23} that can be excited with a bichromatic laser field, as a function of the ratio of the two Rabi frequencies Ω_{12}/Ω_{13} according to Eq. (9). The excitation efficiency is highest if both optical Rabi frequencies are identical.

In close analogy to the doubly resonant case one can obtain an analytical solution for the sublevel coherence at the end of the excitation period. When we separate the real and imaginary parts of the coherence, $\rho_{23}(t)=x_{23}(t)+iy_{23}(t)$, we find

$$x_{23}(t)=\frac{1+\cos\Theta}{16}\left[(\cos\Theta-3)\cos\Omega_0 t+4(1-\cos\Theta)\cos\left[\frac{\Omega_0}{2}t\right]-1+3\cos\Theta\right], \tag{12}$$

$$y_{23}(t)=\frac{1+\cos\Theta}{4}\left[-\sin\left[\frac{\Theta}{2}\right]\sin\Omega_0 t+2\sin\left[\frac{\Theta}{2}\right]\sin\left[\frac{\Omega_0}{2}t\right]\right].$$

The coherence contains a time-independent term, as well as terms oscillating at the effective Rabi frequency Ω_0 and its subharmonic $\Omega_0/2$.

To get an idea how the efficiency of the excitation process depends on the frequency mismatch δ_m, we consider the common prefactor

$$\frac{1+\cos\Theta}{4}=\frac{\Omega_1^2}{2\Omega_1^2+\delta_m^2}, \tag{13}$$

which has a Lorentzian dependence on the frequency mismatch δ_m. As expected, the amplitude reaches its maximum at resonance. If the detuning exceeds the Rabi frequency Ω_1, the amplitude of the sublevel coherence decreases.

In the case of bichromatic excitation, it is always possible to maximize the excitation efficiency by setting the frequency difference to the sublevel splitting, $\omega_m=\Delta$. In the case of the conventional monochromatic excitation, however, where $\omega_m=0$, the frequency mismatch δ_m becomes equal to the sublevel splitting Δ. According to Eq. (13) the excitation efficiency decreases if this sublevel splitting exceeds the optical Rabi frequency.

This decrease of the excitation efficiency can be compensated partially, if one increases the optical Rabi frequency using higher laser intensities. With typical commercially available cw lasers, however, the available power limits the Rabi frequency in rare-earth solids to well below 1 MHz, making the excitation rather inefficient in systems with splittings above 1 MHz.[11] Another possibility is the use of short laser pulses: the excitation bandwidth increases with the inverse of the pulse duration. However, since the sublevel coherence increases with the square of the pulse duration, the amplitude of the coherence remains small for short pulses of limited Rabi frequency.

D. Detection of sublevel coherence

For a discussion of the detection process we refer to Fig. 4. After the end of the excitation period the bi-

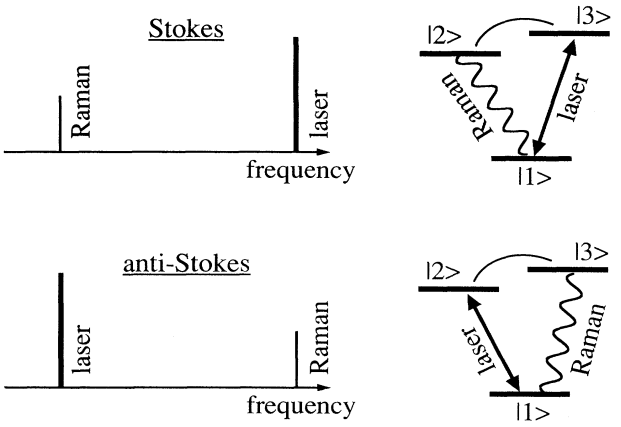

FIG. 4. Schematic representation of the coherent Raman scattering process. A resonant test laser beam is Raman scattered from the coherence between sublevels $|2\rangle$ and $|3\rangle$. The frequency difference between the scattered Raman field and the incident test laser field corresponds to the sublevel transition frequency. Depending on the frequency of the test laser beam, either Stokes (upper case) or anti-Stokes Raman scattering (lower case) can be observed.

chromatic laser field has created a coherent superposition $\rho_{23}(t)$ of sublevels $|2\rangle$ and $|3\rangle$. This coherence is detected with a near-resonant test laser field of amplitude E_T, which couples to one of the optical transitions, e.g., to transition $|1\rangle\leftrightarrow|3\rangle$, and scatters off the sublevel coherence in the adjacent transition $|2\rangle\leftrightarrow|3\rangle$ in a coherent Raman scattering process.[1,14] When the scattered Raman field and the test laser field are superimposed on a photodetector, their interference can be detected as a beat signal

$$S(t)=\text{const}\times E_T^2[\mu_{13}\mu_{21}\rho_{32}(t)+\text{c.c.}]\ . \tag{14}$$

The signal is linear in the intensity of the incident test laser field and in the product of the dipole matrix elements of both optical transitions that are involved in the Raman scattering process. The Raman beat signal is directly proportional to the coherence ρ_{23} and monitors its evolution. We expect therefore an oscillation at the sublevel transition frequency and a decay at its damping rate. The signal frequency is independent of the laser frequency and therefore not affected by the laser frequency jitter.

As is shown in the upper part of Fig. 4 the coherent Raman scattering process generates a field in the second optical transition $|1\rangle\leftrightarrow|2\rangle$, whose frequency is lower than that of the incident test laser field. In this case, we deal with a Stokes process. However, this asymmetry between Stokes and anti-Stokes processes is imposed by the choice of the laser frequency, not by the scattering process itself, which has equal cross sections for both processes,[1] as Eq. (14) shows. By tuning the laser frequency to the transition $|1\rangle\leftrightarrow|2\rangle$ we can excite the anti-Stokes process, for which the Raman field couples to the transition $|1\rangle\leftrightarrow|3\rangle$, as shown in the lower part of Fig. 4.

IV. EXPERIMENTAL SETUP

The experiments were performed in a Pr^{3+}:$YAlO_3$ (YAP) crystal with a Pr^{3+} concentration of 0.1%. For triply ionized rare-earth ions in crystal fields, optical transitions between levels of the same $4f^N$ configuration are only weakly dipole allowed.[15] This is the reason for the very narrow homogeneous optical linewidths that can be observed in these systems. The optical transition between the $^3H_4$ electronic ground state and the $^1D_2$ excited state of Pr^{3+}:YAP has an oscillator strength of 10^{-7}.[16] Typical optical Rabi frequencies are therefore in the kilohertz range.

The interaction of the electric quadrupole moment of the ^{141}Pr nucleus ($I=\frac{5}{2}$) with the electric field gradient at the ion site lifts the degeneracy of the nuclear spin sublevels. The left-hand part of Fig. 5 shows the relevant part of the energy-level scheme for the $^3H_4$ ground and the $^1D_2$ excited state of Pr^{3+}:YAP. The two electronic states split into three doubly degenerate pairs of sublevels with magnetic quantum numbers $m_I=\pm\frac{1}{2}$, $\pm\frac{3}{2}$, and $\pm\frac{5}{2}$. The residual degeneracy can be lifted when an external magnetic field is applied to the sample. The energy separations between these sublevels are 0.9, 1.6, and 2.5 MHz in the in the excited state and 7, 14.1, and 21.1 MHz in the electronic ground state. The orientation of the quadrupole tensors of the ground and excited states differs by 12.8°.[17] The different orientation of the quantization axes in ground and excited states makes all electric dipole matrix elements between nuclear spin states of the electronic ground and excited states nonzero. The system includes therefore several three-level systems in which coherent Raman beats can be excited.

To satisfy the double-resonance condition the frequency difference between both components of the bichromatic laser field has to be equal to the sublevel transition frequency. We use intensity modulation of the output of a single laser beam to generate the two frequency components. We have used electro-optic and acousto-optic modulators for this purpose, but describe here explicitly only the case of an acousto-optic modulator (AOM). In this case, we modulate the carrier frequency ω_c of the AOM with a modulation frequency ω_m, creating sidebands at $\omega_c\pm\omega_m/2$. As the frequency of the laser field is shifted by the frequency of the acoustic wave during the inelastic scattering process in the modulator, the two modulation sidebands of the rf field give rise to two frequency-shifted beams. If both diffracted beams are imaged onto the sample, the total electric field

$$E(t)=\frac{E_0}{2}[e^{i(\omega_L+\omega_c+\omega_m/2)t}+e^{i(\omega_L+\omega_c-\omega_m/2)t}] \tag{15}$$

contains two modulation sidebands. The intensity of the pump beam is then modulated sinusoidally,

$$I(t)=\tfrac{1}{2}E_0^2[1+\cos\omega_m t]^2 \tag{16}$$

at the modulation frequency ω_m. The double-resonance condition for the excitation of coherence is satisfied for $\omega_m=\Delta$.

Figure 6 shows schematically the experimental setup.

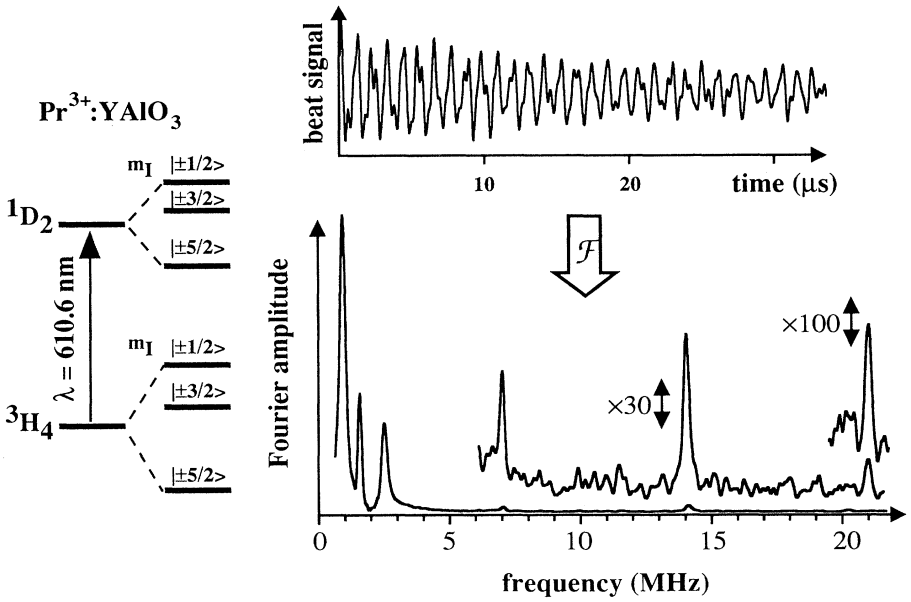

FIG. 5. The left-hand side shows the energy-level scheme of Pr^{3+}:$YAlO_3$. The hyperfine structure of the ground and the excited states contains three doubly degenerate nuclear spin sublevels with different magnetic quantum numbers. The signal shows a coherent Raman beat, which was excited with a short laser pulse (τ=0.9 μs). Its Fourier transform contains resonance lines at all six sublevel splittings.

The crystal was mounted on the cold finger of a helium flow cryostat. Pump and test laser beam were derived from the same laser. Both linearly polarized beams propagated along the crystallographic c axis at an angle of intersection of 5 mrad and were focused with an $f=+300$ mm lens onto the sample. The frequency of the actively stabilized ring dye laser (Spectra Physics 380D) was set to the center of the inhomogeneously broadened absorption line at a wavelength of 610.6 nm. For the smaller sublevel splittings in the excited state, the bichromatic laser field was realized by intensity modulation of the pump beam pulses with an acousto-optic modulator (AOM1) as discussed. For the larger sublevel splittings in the ground state we used an electro-optic modulator (not shown in the figure) between two crossed polarizers.

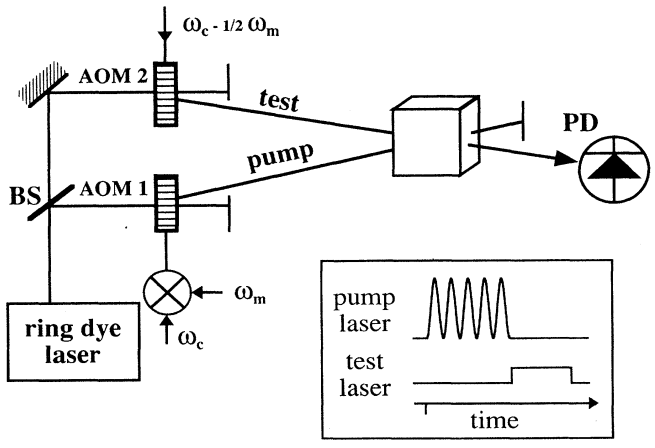

FIG. 6. Experimental setup. BS=beam splitter, AOM=acousto-optic modulator, ω_c and ω_m=carrier and modulation frequency of the rf field, which drives AOM 1, PD=photodiode. The inset shows the time dependence for the intensities of pump and test laser beams.

The inset of Fig. 6 shows the timing in the experiment. During the sample excitation the intensity of the pump laser beam is modulated sinusoidally and is gated by AOM1 which produces pulses with a duration of 0.1–100 μs at typical intensities of 200–300 mW/mm^2. After the end of the pump pulse, the second acousto-optic modulator (AOM2) switches on a weaker test laser beam (<1 mW/mm^2). The rf synthesizer, which drives AOM2, is tuned close to one of the two modulation sidebands of the rf field, which drives AOM1. The beat signal between the test laser and the scattered Raman field is detected with a fast photodiode. This time-domain signal is averaged on a digital storage oscilloscope and is then Fourier transformed on a computer to obtain the spectrum. After each cycle both laser beams were switched off, so that the system could relax towards thermal equilibrium before the next pump pulse. To avoid spectral hole burning in the sample by the repetitive excitation pulses, the temperature of the crystal was set to 8 K, where the spin relaxation rates in the crystal[18] allowed a repetition rate of 50 Hz.

V. EXPERIMENTAL RESULTS

A. Excitation efficiency

Before we discuss in detail the experimental results of the bichromatic excitation scheme, we present results obtained with the conventional monochromatic excitation scheme.[11] For this purpose, we used a pump laser intensity of 1.3 W/mm^2 and excited sublevel coherence with a monochromatic pulse. Variation of the pulse duration gave a maximum of the excitation efficiency for a duration of $t\sim0.9$ μs. Figure 5 (right-hand side) shows a typical Raman beat signal that was obtained with this technique, consisting of 500 accumulated transients. Fourier

transformation of this time-domain signal yielded the spectrum shown at the bottom. The spectrum contains resonance lines at the resonance frequencies of all six sublevel transitions. The three low-frequency lines represent transitions in the excited state, while the three resonance lines at 7, 14.1, and 21.1 MHz are ground-state transitions. The spectrum shows clearly a large decrease in signal intensity at higher frequencies. This intensity decrease is in good agreement with the theoretical prediction of Eq. (13): we expect it to occur whenever the sublevel splitting exceeds the optical Rabi frequency. This is the reason that these transitions could not be observed before.[11]

With a bichromatic laser field this limitation can be overcome. When the bichromatic laser field is realized by intensity modulation, the double-resonance condition is satisfied if the modulation frequency matches the corresponding sublevel transition frequency. Six independent experiments are therefore required to observe all sublevel splittings that exist in the ground and in the excited state of Pr:YAP. Figure 7 shows the Fourier transforms of six Raman beat signals that were excited with modulated laser pulses at a mean laser intensity of 0.6 W/mm^2. For the excited-state spectra the intensity modulation was performed with an AOM and for the ground-state spectra, where the sublevel splittings are larger, with an electro-optic modulator (EOM) between crossed polarizers. The nearly equal peak intensities in the spectra show that the amount of coherence which can be excited becomes practically independent from the sublevel splittings, when a bichromatic laser field is used for the excitation.

The observed Raman beat signal is directly proportional to the sublevel coherence. In particular, the phase of the signal reflects the phase of the sublevel coherence. The excitation process creates the sublevel coherence with a phase that depends on the relative phase difference of the two frequency components. In our experimental setup, this phase is determined by the phase of the modulation frequency. Shifting the modulation phase shifts the phase of the signal by the same amount. This behavior is particularly important when signal averaging is used. In this case, the excitation pulse must always start with the same phase, since the signal averages to zero otherwise.

B. Test laser frequency

When the sublevel splitting exceeds the optical Rabi frequency, a precise control of the laser frequency is important not only for the excitation, but also for the detection of coherent Raman beats. As the bichromatic laser field excites only those atoms from the inhomogeneously broadened absorption line which are simultaneously resonant with both optical frequencies, the test laser beam can only detect the sublevel coherence if it couples to these excited atoms. Hence the test laser frequency must match the frequency of one modulation sideband of the pump beam. To demonstrate this, we measured the amplitude of the coherent Raman beat signal as a function of the frequency difference between test and pump laser beams.

For this purpose, we excited a coherent superposition of the $|\pm\frac{3}{2}\rangle$ and $|\pm\frac{5}{2}\rangle$ nuclear spin sublevels of the electronic ground state by modulating the intensity of the pump laser pulses at a frequency of 14.1 MHz. The upper part of Fig. 8 shows schematically the frequency spectrum of the pump laser field which contains two modulation sidebands at ± 7.05 MHz around the mean laser frequency ν_L of the pump beam. To match the two frequencies, we tuned the test laser frequency through the carrier frequency which drives the acousto-optic modulator AOM2 in Fig. 6. The lower part of Fig. 8 shows the amplitude of the coherent Raman beat signal as a function of the difference between the test laser frequency and the mean frequency of the pump laser beam.

The experiment shows that the beat signal is only observable within a narrow region around both modulation

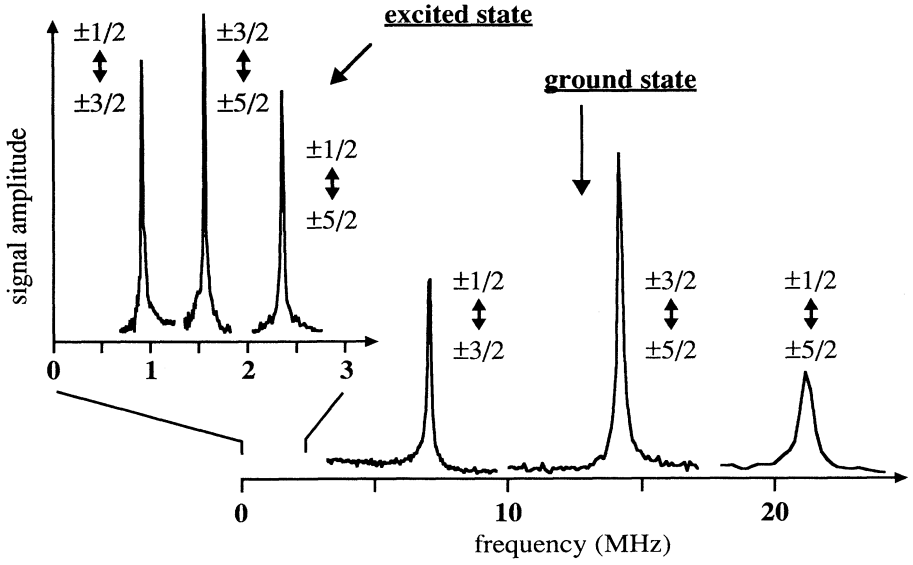

FIG. 7. Fourier transforms of six different Raman beats obtained with bichromatic excitation. The Fourier transforms show the six sublevel transitions. For each spectrum the modulation frequency was in resonance with one sublevel transition.

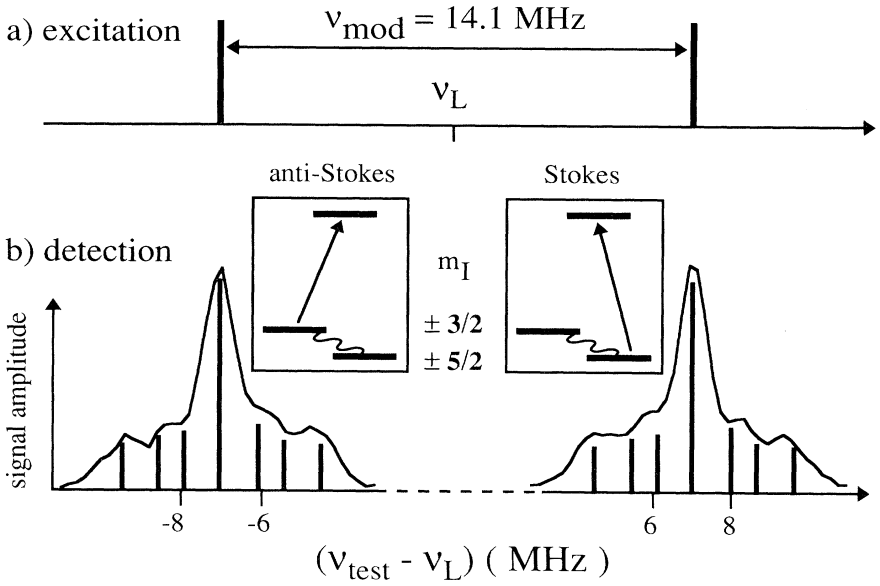

FIG. 8. (a) Frequency spectrum of the pump laser beam if the intensity is fully modulated at frequency ν_{mod}. It contains two modulation sidebands at $\nu_L \pm \nu_{mod}/2$. (b) Amplitude of the Raman beat signal as a function of the difference $\nu_{test} - \nu_L$ between the test and the mean pump laser frequency. The stick spectrum shows the optical resonance frequencies, taking the sublevel splittings of the excited state into account.

sidebands. The width of the peaks near the two sidebands is of the order of 1 MHz and corresponds to the laser frequency jitter. Therefore the accuracy for controlling the test laser frequency has to be only of the same order of magnitude. The broad wings of the signal amplitude around both modulation sidebands at ±7.05 MHz are due to the partially resolved hyperfine structure in the electronically excited state. For Pr:YAP the corresponding sublevel splittings are ±0.9, ±1.6, and ±2.5 MHz as indicated by the sticks in the spectrum of Fig. 8.

The two insets in Fig. 8 show that the test laser beam couples to different optical transitions for each of the two peaks. For the left peak at $\nu_{test} - \nu_L = -7.05$ MHz the test laser beam couples to the optical transition between the $m_I = \pm\frac{3}{2}$ sublevel and the excited state. As the frequency of the scattered Raman field is higher than that of the incident test laser field, the scattering process is in this case an anti-Stokes Raman process. For the right peak at +7.05 MHz the test laser field couples to the optical transition between the $m_I = \pm\frac{5}{2}$ sublevel and the excited state. In this configuration coherent Stokes Raman scattering gives rise to the beat signal. In the experiment the two scattering processes can be separated by tuning the test laser frequency. According to Eq. (14), both scattering processes have the same cross section and yield the same signal amplitude, in agreement with the experiment.

C. Modulation-frequency dependence

The frequency difference between the two components of the bichromatic laser field is an additional degree of freedom in the experiment. If the bichromatic laser field is realized by intensity modulation of the pump pulses, this frequency difference can be adjusted by tuning the modulation frequency. When it equals the sublevel transition frequency, both components of the bichromatic laser field can be in resonance with an optical transition of the three-level atom, which yields the highest excitation efficiency.

For a measurement of the modulation-frequency dependence, we used the $\pm\frac{3}{2} \leftrightarrow \pm\frac{5}{2}$ nuclear spin transition of the excited state with a splitting of 1.56 MHz. For a given pulse length the modulation frequency was varied for successive experiments in the range between 1.2 and 2.0 MHz, using a pump intensity of 0.3 W/mm^2. The beat signal was Fourier transformed and the Fourier amplitude at the sublevel transition frequency was measured. The data points in Fig. 9 show the observed Fourier amplitude for four different pulse lengths as a function of the modulation frequency. When the modulation frequency matches the energy separation between the two excited-state sublevels, the amplitude of the beat signal is largest, as predicted by the theory. Besides the central resonance line, characteristic side peaks occur in the spectrum, whose position depends on the pulse duration. Under our experimental conditions, the amplitude of these side peaks was always smaller than that of the central peak.

For a comparison of these experimental with theoretically expected data, we calculated the amplitude of the density matrix element ρ_{23} after the end of a pump pulse of length τ. As a parameter in the numerical simulation we chose an optical Rabi frequency of 15 kHz, which agrees with published data.[19] To calculate the ratio of the transition strengths of the two optical transitions, we assumed that electronic and nuclear wave functions are separable in the ground and in the excited state, as proposed by Mitsunaga, Kintzer, and Brewer.[17] The relative transition strength can then be obtained from the overlap integral between corresponding nuclear spin eigenfunctions of the ground and the excited state. In a first calculation we assumed that the laser detuning $\delta_L = \omega_0 - \omega_L$ between the mean optical transition frequency ω_0 and the mean frequency ω_L of the pump laser field (see Fig. 2) vanishes. The resulting amplitude for a pulse length of 10 μs is superimposed as a dashed line on the experimental data points in Fig. 9. Obviously, the width of the cen-

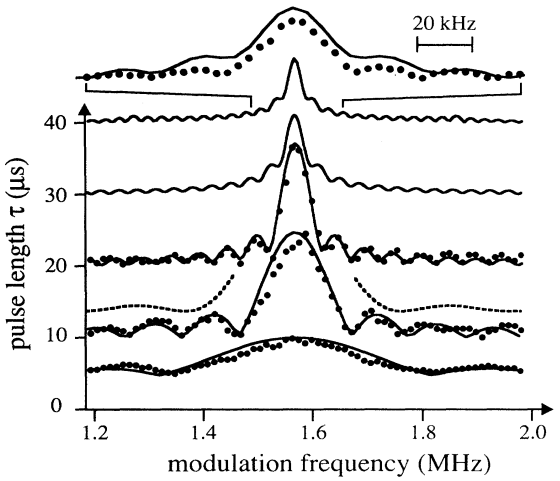

FIG. 9. Dependence of the Raman beat signal on the modulation frequency as a function of the pulse length τ. The points represent the observed amplitude of the Raman beat signal. The solid lines show the theoretically expected values for the sublevel coherence ρ_{23}, taking the laser frequency jitter into account. The trace at the top shows the central part of the data at $\tau=40$ μs on an extended scale and the dashed line the theoretical value for a laser with no frequency jitter.

tral peak is significantly larger than for the experimental data and the position of the side peaks does not agree with the experiments.

This disagreement is associated with the assumption that the laser has an ideal frequency stability. However, in the experiments the laser frequency jitter (0.5 MHz) was much larger than the homogeneous linewidth of the optical transitions [5 kHz (Ref. 16)] or the optical Rabi frequency. As a consequence, pump and test laser pulses were not always in resonance with the same atom during the preparation and detection period. In this case, the transformation (4) to the rotating frame must use the laser frequency ω_L, which may differ from the atomic resonance frequency ω_0. The rotating-frame Hamiltonian is then

$$\mathcal{H}'=\begin{pmatrix} -\frac{2\delta_L}{3} & \frac{\Omega_{12}}{2} & \frac{\Omega_{13}}{2} \\ \frac{\Omega_{12}}{2} & \frac{\delta_L}{3}-\frac{\delta_m}{2} & 0 \\ \frac{\Omega_{13}}{2} & 0 & \frac{\delta_L}{3}+\frac{\delta_m}{2} \end{pmatrix}, \tag{17}$$

where the laser frequency detuning is δ_L. In atoms that are detuned from the laser frequency, the coherence builds up faster but saturates at a lower level.

As a result of the laser jitter, the probe laser is resonant with several groups of atoms for which the pump laser had different detunings during excitation. For a numerical calculation of the system dynamics we assumed that all atoms whose resonance frequencies were within the range of the laser frequency jitter were detected with the same sensitivity. The traces that are superimposed on the experimental data in Fig. 9 represent the calculated amplitude $|\rho_{23}|$ of the sublevel coherence. Each trace represents the numerical average over a distribution of 301 atoms whose resonance frequencies varied from $\delta_L=-300$ to 300 kHz. Comparison with experimental data shows that this simulation yields the same dependence of the central peak width on the pulse length and of the side peak positions on the modulation frequency.

A comparison of the data for different pulse durations shows that the sublevel coherence reaches its maximum at $\tau=20$ μs, which corresponds to a quarter period of the Rabi frequency. With increasing pulse length, the width of the central resonance line decreases in inverse proportion to the pulse length until it approaches a value of 20 kHz, which is of the order of the optical Rabi frequency. The trace at the top of the figure, which displays the central part of the data with a pulse duration of 40 μs, shows this in detail. These data demonstrate again why monochromatic excitation yields only small signals: To obtain a good excitation over a large frequency range, short pulses are required. On the other hand, the excitation reaches its maximum only after some 20 μs.

VI. DISCUSSION

To the best of our knowledge, all coherent Raman beat experiments that have been performed so far on rare-earth solids have used short monochromatic laser pulses to excite coherence between two sublevels, which is required for the coherent Raman scattering process. However, the experiments showed the limitations of this excitation method, as a monochromatic laser field cannot simultaneously couple to two optical transitions of a multilevel atom when the sublevel splitting is larger than the optical Rabi frequency. The method of coherent Raman beats was therefore limited to the spectral range of a few megahertz in these systems.[7]

This limitation can be overcome by using a bichromatic laser field for the excitation. Such a field can be simultaneously resonant with both relevant optical transitions and allows therefore a longer interaction time. Experimentally, we have realized the bichromatic laser field through intensity modulation. Intensity modulation of laser pulses has also been used successfully for coherent sublevel spectroscopy on atomic vapors.[20–22] However, the specific properties of rare-earth ions in solids require a modified experimental procedure. The main differences between the two systems are the strength of the optical transitions and the homogeneous linewidths, which are in the kilohertz range for rare-earth ions, but in the gigahertz range for pressure-broadened atomic vapors.

The small transition strengths of optical transitions in rare-earth solids correspond to small Rabi frequencies, which limit the spectral range for the monochromatic excitation. The small linewidths of the optical transitions require accurate control of the frequencies of the laser fields that are involved in the excitation and the detection process. In our experimental setup, we use radio frequency sources for the control of these parameters: the modulation frequency determines the frequency difference between the two laser fields during the excitation and the

double-resonance condition is satisfied if this modulation frequency is equal to the sublevel transition frequency. For the detection, we used an acousto-optic modulator to shift the test laser frequency to a modulation sideband of the pump beam.

To describe the excitation process theoretically, we used a model based on three-level atoms. It assumes that both frequency components of the bichromatic laser field couple to only one optical transition. Hence this model is especially suited to describe the bichromatic excitation in multilevel atoms, when the optical Rabi frequency is smaller than the sublevel splittings. The comparison of its predictions with experimentally observed data shows that the model agrees qualitatively and quantitatively with the observed behavior. The model is related to calculations of multiphoton processes in three-level atoms[23–25] of multilevel atoms,[26] which discuss the optimum conditions for the selective transfer of population to certain states of a multilevel atom.

For optimal excitation of sublevel coherence, the two optical Rabi frequencies must be equal: $\Omega_{12}=\Omega_{13}$. In our setup, where we modulated the intensity of the pump beam, the amplitudes of both sidebands are equal. A maximum excitation efficiency can then only be obtained if the dipole matrix elements for the two optical transitions are equal. This might cause problems in coherent Raman beat experiments on other systems, where the ratio of the transition strengths is less favorable than for Pr:YAP. However, the bichromatic laser field offers an additional degree of freedom to the experimenter to increase the excitation efficiency. It is possible to choose different amplitudes for the two frequency components, thus optimizing the efficiency for arbitrary ratios of dipole matrix elements.

In our model system Pr:YAP, we have observed coherent Raman beats over a range of 1–21 MHz, using optical Rabi frequencies of less than 100 kHz, thus demonstrating that it is possible to excite wide spectra with low-power lasers, even if the transition strengths are weak. The spectral range over which this method is applicable is not limited to these frequencies. Using faster modulators, it could be extended into the gigahertz range. Furthermore, it should be possible to use the output of two independent laser sources, if the frequency difference between the two lasers can be kept stable enough during the sample preparation.

ACKNOWLEDGMENTS

We thank Professor J. Mlynek for generously lending us the crystal, Stefan Altner for helpful discussions, and the Schweizerischer Nationalfonds for financial support.

[1]J. A. Giordmaine and W. Kaiser, Phys. Rev. **144**, 676 (1966).
[2]N. Wong, E. Kintzer, J. Mlynek, R. De Voe, and R. Brewer, Phys. Rev. B **28**, 4993 (1983).
[3]H. Burggraf, M. Kickartz, and H. Harde, in *Methods of Laser Spectroscopy,* edited by Y. Prior, A. Ben-Reuven, and M. Rosenbluth (Plenum, New York, 1986).
[4]R. G. De Voe and R. G. Brewer, Phys. Rev. Lett. **40**, 862 (1978).
[5]J. P. Heritage, T. K. Gustafson, and C. H. Lin, Phys. Rev. Lett. **34**, 1299 (1975).
[6]A. Z. Genack and R. G. Brewer, Phys. Rev. A **17**, 1463 (1978).
[7]R. M. Shelby, A. C. Tropper, R. T. Harley, and R. M. MacFarlane, Opt. Lett. **8**, 304 (1983).
[8]R. Yano, M. Mitsunaga, and N. Uesugi, Opt. Lett. **16**, 1884 (1991).
[9]M. Mitsunaga, R. Yano, and N. Uesugi, Opt. Lett. **16**, 1890 (1991).
[10]S. Völker, Annu. Rev. Phys. Chem. **40**, 499 (1989).
[11]R. M. Shelby and R. M. MacFarlane, J. Lumin. **31&32**, 839 (1984).
[12]T. Blasberg and D. Suter, Opt. Commun. **109**, 133 (1994).
[13]L. Allen and J. H. Eberly, *Optical Resonance and Two-Level Atoms* (Wiley, New York, 1975).
[14]R. G. Brewer and E. L. Hahn, Phys. Rev. A **8**, 464 (1973).
[15]S. Hüfner, *Optical Spectra of Transparent Rare Earth Compounds* (Academic, New York, 1978).
[16]R. M. MacFarlane and R. M. Shelby, in *Spectroscopy of Solids Containing Rare Earth Ions,* edited by A. Kaplyanskii and R. M. MacFarlane (North-Holland, Amsterdam, 1987).
[17]M. Mitsunaga, E. Kintzer, and R. Brewer, Phys. Rev. B **31**, 6947 (1985).
[18]T. Blasberg and D. Suter, Chem. Phys. Lett. **215**, 668 (1993).
[19]R. M. MacFarlane, R. M. Shelby, and R. L. Shoemaker, Phys. Rev. Lett. **43**, 1726 (1979).
[20]W. E. Bell and A. L. Bloom, Phys. Rev. Lett. **6**, 280 (1961).
[21]H. Lehmitz, W. Kattau, and H. Harde, in *Methods of Laser Spectroscopy* (Ref. 3).
[22]D. Suter and J. Mlynek, Phys. Rev. A **43**, 6124 (1991).
[23]K. Bergmann, in *Atomic Physics 12,* edited by Jens C. Zorn and Robert R. Lewis, AIP Conf. Proc. No. 233 (AIP, New York, 1991).
[24]C. E. Carroll and F. T. Hioe, J. Opt. Soc. Am. B **5**, 1335 (1988).
[25]J. R. Kulinski, U. Gaubatz, F. T. Hioe, and K. Bergmann, Phys. Rev. A **40**, 6741 (1989).
[26]J.-C. Diels and S. Besnainou, J. Chem. Phys. **85**, 6347 (1986).